Field Crops Research 299 (2023) 108977

Contents lists available at ScienceDirect

Field Crops Research

journal homepage: www.elsevier.com/locate/fcr

Modelling potato yield losses caused by *Phytophthora infestans:* Aspects of disease growth rate, infection time and temperature under climate change

José González-Jiménez [a,*], Björn Andersson [a], Lars Wiik [b], Jiasui Zhan [a]

[a] Department of Forest Mycology and Plant Pathology, Swedish University of Agricultural Sciences, Uppsala, SE-75007 Uppsala, Sweden
[b] Department for Research and Development, The Rural Economy and Agricultural Society, Scania, Sweden

ARTICLE INFO

Keywords:
Late blight
Damage mechanism
Scenario analysis
Apparent infection rate
Temperature response function
System dynamics

ABSTRACT

Modelling crop yield loss due to pathogens remains a challenge due to the complex and dynamic interactions involved. Here, we develop a parsimonious dynamic yield loss simulation model that couples a simple epidemiological model of late blight disease with a basic model of potato crop growth. The model is parameterized using 17 years of field data on disease progress of potato late blight and potato yield in southern Sweden. Simulated actual yields (yields obtained under the presence of *Phytopthora infestans*) correlated well ($R^2 = 0.66$) with the actual yields observed in field trials, using a few widely accessible meteorological variables. The results also underline the impact of disease growth rate and the time of infection on yield losses, with relatively low rates and early onset of the epidemic producing large yield reductions. In addition, the importance of increasing temperature due to climate change on both potato crop and *Phytophthora infestans* development was simulated, suggesting that higher temperatures may be more detrimental for the pathogen than for the crop. Additional ways to expand the model are discussed, and the inclusion of other diseases and pests are encouraged, indicating the potential to improve disease management in potato production.

1. Introduction

Increased food security is at the heart of the UN 2030 Agenda for sustainable development (IPBES, 2019; UN, 2015). However, the growth in global population, the depletion of vital natural resources used in agriculture and environmental stress associated with the ongoing climate change undermine the achievement of this goal. Primary food production must be increased without use of additional resources such as energy and arable land (Davis et al., 2016; Godfray et al., 2010). In addition, crop pests and diseases (CPDs) cause up to 40% production loss in some of the major crops at global scale, constantly jeopardizing food security (Savary et al., 2019). One of the most sustainable ways to improve agricultural productivity is to reduce the substantial yield losses caused by CPDs. This could be achieved by formulating better integrated pest management approaches that support a reduction in chemical inputs in line with eco-evolutionary principles (Burdon et al., 2019; He et al., 2021b, 2021a; Zhan et al., 2015).

Modelling agricultural systems has been extensively used over the last decades to better understand the contribution of different components (production, land use, natural resources, diseases and human factors) and their complex interactions to primary production (Jones et al., 2017). In addition, climate change is affecting both crop productivity and plant disease epidemiology. The impacts on crop production from these two factors are intertwined and hard to separate and therefore modelling is an important tool to facilitate the design and adoption of efficient disease control strategies (Juroszek and von Tiedemann, 2015).

Until recently, statistical models, based on empirical relationships between yield and environmental factors over several experimental observations in a specific location or region, have been the dominant approach when it comes to assessing yield losses (Jones et al., 2017). However, these models tend to have a limited use when they are applied in locations with environmental conditions different from those where the models were originally developed (Donatelli et al., 2017). This becomes especially troublesome under the ongoing climate change, since a statistical model developed under specific environmental conditions may become of no or little use even in the same location/region where it was developed. An alternative approach is the use of mechanistic, process-based models that rely on the characterization of fundamental and dynamic physical and biochemical interactions between the crop and its abiotic and biotic environment (Donatelli et al., 2017; Esker et al., 2012).

* Corresponding author.
E-mail address: jogonji82@gmail.com (J. González-Jiménez).

https://doi.org/10.1016/j.fcr.2023.108977
Received 10 June 2022; Received in revised form 9 May 2023; Accepted 18 May 2023
Available online 29 May 2023

Mechanistic simulation models have become important tools to quantitatively improve our knowledge of complex biological systems such as crop-pathogen-environment systems by integrating the knowledge derived from decades of empirical research into key processes and mechanisms that determine the behaviour of the system of interest (Wallach et al., 2019). Because of this integrating and assimilatory capacity, mechanistic models are able to simplify the complexity that characterizes the interplay between crops, the environment and their pests and diseases. Simulating crop losses through mechanistic models allows the quantification of damages caused by one or several stressors (biotic and/or abiotic) in a given agroecosystem (Donatelli et al., 2017; Esker et al., 2012; Savary et al., 2018), thus enabling the adoption of tactical (as part of decision support systems; Isard et al., 2015, Magarey et al., 2002) and strategic decisions for disease and pest management (van Oijen, 1992; Willocquet et al., 2004). Paramount in this type of modelling is the concept of damage mechanisms, i.e., in what way a given harmful organism (CPDs and also weeds) affects the host plant's physiological status to support its growth and development (Boote et al., 1983; Gaunt, 1995; Rouse, 1988).

Potato is among the most important food crops in the world in terms of human consumption (Devaux et al., 2020). However, potato production is continually threatened by both abiotic factors (soil fertility, water supply, frosts and droughts) and biotic factors (CPDs), the latter causing up to 20% losses of the global potato production (Savary et al., 2019). The oomycete *Phytophthora infestans* (Mont.) de Bary, the causal agent of the late blight disease in potato, is considered to be the most harmful pathogen in potato crops due to its rapid evolution, high adaptability and short epidemic cycle (Leesutthiphonchai et al., 2018). Potato late blight was one of the main factors involved in the infamous famine in Ireland in the mid nineteenth century (Bourke, 1955; Yoshida et al., 2013). Under favourable weather conditions, *P. infestans* can destroy the entire canopy of a potato crop within 10–15 days, resulting in total yield losses (Rakotonindraina et al., 2012). Because of this, late blight control today largely relies on repeated fungicide applications. This dependence has detrimental effects on the environment, and greatly threatens agricultural sustainability.

Many potato growth models are currently available. However, the majority of these models only describe the direct impacts of abiotic factors on the growth and development of the potato plants and the associated yield losses, but overlook the effects of biotic CPDs on yield reduction (Raymundo et al., 2014). Only very few potato agro-physiological models have incorporated CDPs routines in their structure. For example, Johnson (1992) incorporated two diseases and one pest in a potato growth model, but did not include the effect of *P. infestans*. Kaukoranta (1996) and Rakotonindraina et al. (2012) simulated potato yield losses caused by *P. infestans,* but the pathogen's damage mechanisms was only partially characterized. On the other hand, van Oijen (1992) and Skelsey et al., (2010, 2009a, 2009b) used more comprehensive approaches to characterize the damage mechanisms of *P. infestans* on potatoes. However, limitations in the empirical modelling used to represent potato growth confine the extrapolation of their forecasts.

These modelling gaps in the characterisation of potato yield loss constitute the rationale for the work presented here. The objectives of this study were to (i) develop and test a flexible, user-friendly and simplified mechanistic model for the assessment of potato yield losses caused by *P. infestans* as a primary pathogen on this crop, (ii) determine the importance of the rate of disease growth and the time of the onset of the epidemic on the yield reduction caused by *P. infestans,* and (iii) evaluate the model sensitivity to changes in meteorological variables in relation to near-future climatic change. The ultimate aim is to develop and validate an accessible potato yield loss model that can be used to improve current integrated pest management (IPM) strategies against late blight by incorporating other biotic (i.e., emerging diseases) and abiotic (i.e., environmental factors) for a more sustainable global food production.

2. Material and methods

2.1. Field trials and database

The yield loss simulations and statistical analyses conducted in this study were based on a database consisting of 71 field trials performed in three different locations (Lilla Böslid, Mosslunda and Borgeby) in southern Sweden during 1993–2017. Treatments in the field trials comprised different fungicide application programs with the objective to test their efficacy in controlling *P. infestans*. Certified seed of the cultivar Bintje, a cultivar that is highly susceptible to late blight, was used in all trials. Standard agronomical practices were followed, including compound fertiliser and manganese applications, irrigation, and control of weeds, insect pests and early blight (*Alternaria solani*).

In each trial, basic agronomical data such as date of planting, 100% plant emergence and chemical desiccation was recorded. Date of 50% plant emergence was also recorded in 31 out of the 71 trials. The difference between date of 100% and 50% plant emergence was calculated in these trials and the average was used to estimate the date of 50% plant emergence in the trials where it was not recorded. An untreated control where no fungicides to control late blight were applied was also included in all trials. The yield obtained from the most effective fungicide treatment was considered to represent the attainable yield, that is, the yield produced by a crop free (usually above 99%) of disease, grown with optimal supply of soil nutrients and water (Rabbinge, 1993; Zadoks and Schein, 1979). The yield from the untreated control plots represented the actual yield, and the yield loss was computed as the difference between the attainable and the actual yield. Actual yield here therefore differs from the yield that farmers obtain applying any control measure (e.g., fungicides) to minimize the detrimental effects of CPDs. Recorded yield values, in tons fresh matter ha^{-1}, were converted into grams dry matter m^{-2} using a 20% conversion factor.

Plots were monitored for late blight severity usually once a week during each growing season, generally starting in June. Date of observed disease and its severity (% leaf area infested) was scored following the assessment key by Syrén and Wiik (1993), which is a version adapted to Swedish conditions of the widely used EPPO scale that allows for a more precise estimation of the start of the infection. The same person made all the disease severity assessments across all years and treatments, minimizing variability in the disease assessments. The field trials were naturally infected by local strains of *P. infestans*. A more detailed description of the field trials can be seen in Wiik (2014).

2.2. Model description

2.2.1. General specifications

The model used in this study, named POTATOPEST, is an adapted version of WHEATPEST and RICEPEST, two mechanistic, process-based models originally developed for wheat (Willocquet et al., 2008) and rice (Willocquet et al., 2004, 2002, 2000), respectively. Like its predecessors, POTATOPEST is a simplified simulation model in which only the main agro-physiological processes that define the development of the potato plant are taken into account (such as radiation interception, canopy development, tuber initiation and bulking, etc.), leaving out other processes that contribute little to the behaviour of the system (such as stem population density or canopy architecture) (Savary et al., 2018). At the same time, POTATOPEST allows the incorporation of damage mechanisms caused by one or more potato diseases and/or insect pests. Damage mechanism refers to the physiological processes of the crop that are impaired by a harmful organism (Boote et al., 1983; Savary and Willocquet, 2014). There are two damage mechanisms that *P. infestans* inflict on potato plants; (1) it reduces the green leaf area available for photosynthesis (Bangemann et al., 2014; Haverkort and Bicamumpaka, 1986; Rossing et al., 1992; Waggoner and Berger, 1987); and (2) it accelerates leaf senescence in the remaining, lesion-free area of the leaf, thus indirectly reducing the green leaf area able to intercept radiation

(Bangemann et al., 2014; Skelsey et al., 2009b; van Oijen, 1991a). Hence, the rationale in this model is to compute, as a first stage, the growth, development and yield of the potato plant in absence of injuries caused by *P. infestans* (attainable yield), followed by the quantification of the yield reduction caused by the pathogen (actual yield). The time step in the model is 1 day and the unit of mass (grams) refers to dry matter (DM).

The computation of the growth and development of the potato plant and the effects of pests and diseases is grounded in the principles of stocks, flows, feedbacks and delays of system dynamics theory (Savary and Willocquet, 2014; Sterman, 2000). Stocks represent the amount of important state variables (such as the biomass of the different plant organs) and can only be modified by in-flows (rate at which the stock is increasing over time) and out-flows (the rate at which the stock is decreasing over time). They represent the accumulation (integration) of the net flow and can be expressed as a set of differential equations:

$$\frac{d(stock)}{dt} = inflow(t) - outflow(t)$$

2.2.2. Attainable yield modelling

The main variables of the POTATOPEST model and their units are described in Table 1 and its graphical structure is shown in Fig. 1. A full account of the model variables and details of the equations can be seen in the Supplementary Fig. 1 and Supplementary Table 1, as well as the R script with the code to implement the model. Unlike plant growth, which is a continuous physiological process, the development stage (DS) of the plant refers to the plant age and phenological development, which determines the partitioning of photoassimilates to the different plant organs as well as the natural leaf senescence. The DS variable in POTATOPEST takes discrete unitless values, with 0 at 50% plant emergence, 1 at tuber initiation and 2 at plant desiccation and harvest (Kooman et al., 1996; Penning de Vries and Laar, 1982).

Temperature was considered the only environmental factor driving potato phenological development in POTATOPEST. Short photoperiods (ca. 10 h) promote tuber initiation, while longer photoperiods (ca. 15 h) have little or no effect on plant development (Streck et al., 2007). Therefore, the effect of photoperiod in plant development was not included in POTATOPEST due to the long photoperiods occurring in northern Europe during mid-spring and summer when potato crops are grown (Pulatov et al., 2015).

Development stages (DS) in POTATOPEST are simulated based on growing degree-days, as the sum of effective temperature that the plant needs to accumulate to move from one phenological stage to another. The effective temperature was calculated following a nonlinear function as:

$$ET = \begin{cases} 0, & T_d < T_{\min} \\ \left(\frac{T_d - T_{\min}}{T_{opt} - T_{\min}}\right)\left(\frac{T_{\max} - T_d}{T_{\max} - T_{opt}}\right)^{\left(\frac{T_{\max} - T_{opt}}{T_{opt} - T_{\min}}\right)} (T_{opt} - T_{\min}), & T_{\min} < T_d < T_{\max} \\ 0, & T_d > T_{\max} \end{cases} \quad (1)$$

where ET is the effective temperature, T_d is the daily average temperature obtained from weather stations, and $T_{\min}$, T_{opt} and $T_{\max}$ are the minimum, optimum and maximum temperatures, respectively, that determine the range of temperatures under which potato plant develops, and are set to 2 °C, 22 °C and 35 °C (Pulatov et al., 2015). The use of a nonlinear function offers a realistic description of the relation between growing degree-days and the development rate, as the detrimental effects of temperatures that are above the optimal temperature are taken into account (Zhou and Wang, 2018). Growing degree-days was set to 217 °C-day for the onset of tuber initiation (DS=1) (Kaukoranta, 1996), while for the desiccation and harvest stage (DS=2) it was set as a function of the length of the growing period as follows:

$$GDDM = 134.6 + (12.8 \bullet GS) \quad (2)$$

where, GDDM represents the Growing degree-days at maturity (° C-day), GS is the growing periods (from 50% plant emergence to dessication, in days).

Biomass production is represented in the model as a pool of assimilates (PA) produced daily by the photosynthetic activity, and is based on the Monteith (1977) approach, by which biomass production is proportional to the radiation intercepted by the canopy:

$$GR = PAR \bullet \left(1 - e^{-k \bullet LAI}\right) \bullet RUE \quad (3)$$

where GR is the growth rate, PAR is the photosynthetically active radiation, and was assumed to be 50% of the total radiation reaching the crop canopy (Monteith and Unsworth, 2013), k is the coefficient (constant) of light extinction and was set to 0.55 (Kaukoranta, 1996), RUE is the radiation use efficiency and represents the rate at which the intercepted radiation is converted into biomass (Monteith, 1977).

RUE is considered to be constant when crops are grown under good agronomic conditions (no water nor soil nutrient limitations) (Madden et al., 2007). LAI is the leaf area index and is determined as:

$$LAI = LB \bullet SLA \quad (4)$$

where LB is the leaf biomass and SLA represents the specific leaf area, with a constant value of 0.03 m 2 g-1 (Kabat et al., 1995). The pool of assimilates (PA) is partitioned to the different plant organs (leaves, stems, tubers and roots) on a daily basis (no delay assumed), constituting the leaf biomass (LB), stem biomass (SB), tuber biomass (TB) and root biomass (RB) stocks. Their rates (LA, SA, TA and RA, respectively) at which they are filled are computed as the product of the PA and their coefficients of partitioning (CPL, CPS, CPT and CPR, respectively), which in turn depend on the DS. The values of these coefficients were taken from Kabat et al. (1995), and are available in the Supplementary Table 1.

Table 1
Description of the main variables of the model.

Acronym	Definition	Units[a]	Value
State variable			
PA	Pool of assimilates	g	
LB	Leaf biomass	g	
SB	Stem biomass	g	
TB	Tuber biomass	g	
RB	Root biomass	g	
Flows			
GR	Growth rate	g d^{-1}	
LA	Leaf allocation	g d^{-1}	
SA	Stem allocation	g d^{-1}	
TA	Tuber allocation	g d^{-1}	
RA	Root allocation	g d^{-1}	
LS	Leaf senescence	g d^{-1}	
Auxiliary variables			
DS	Development stage	–	0–2
PAR	Photosynthetically active radiation	MJ m^{-2} d^{-1}	
k	Coefficient of light extinction	–	0.55
LAI	Leaf area index	–	
RUE	Radiation use efficiency	g MJ^{-1}	
SLA	Specific leaf area	m^2 g^{-1}	0.03
CPL	Coefficient of partitioning to leaves	–	f(DS)[b]
CPS	Coefficient of partitioning to stems	–	f(DS)[b]
CPT	Coefficient of partitioning to tubers	–	f(DS)[b]
CPR	Coefficient of partitioning to roots	–	f(DS)[b]
RLS	Rate of leaf senescence	d^{-1}	f(DS)[b]
ST	Carbohydrates in seed tuber	g d^{-1}	1, 0[c]
S	Disease severity of late blight	–	0–1

[a] Biomass units (grams) refer to dry matter;
[b] Values depend on the development stage and are available in the Supplementary Table 1.
[c] Value of ST is 1 g DM for the first 20 days after plant emergence, then 0;

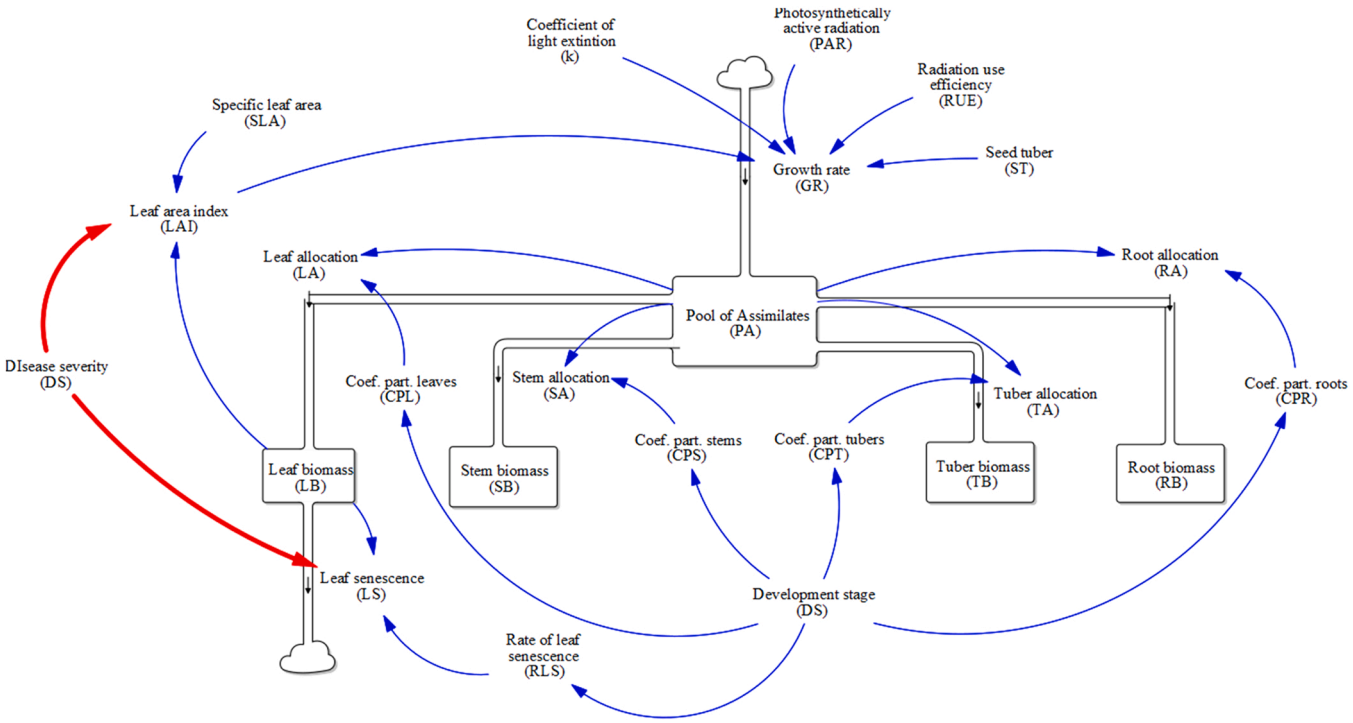

Fig. 1. Simplified stock and flow diagram of POTATOPEST. Stocks (rectangles) represent state variables; flows (material channels joining two rectangles, or rectangle-cloud) are rates of change of state variables with time; blue lines represent information channels which convey information that is not stored; red lines are information channels representing the two damage mechanisms of *P. infestans* on potato plant; clouds are sources or sinks and represent the boundaries of the system.

LB is further modified by the dynamics of natural leaf senescence rate (LS) as follows (Kabat et al., 1995):

$$LS = \begin{cases} LB \cdot RLS, & LAI \le 4 \\ LB \bullet \{RLS + (0.03 \bullet (LAI - 4)/4)\}, & LAI > 4 \end{cases} \quad (5)$$

where *RLS* is the relative rate of leaf senescence and is a function of DS. Eq. 5 accounts for the effect of shelf-shading so that when the plant is fully developed (LAI > 4) the rate of leaf senescence is accelerated due to the lack of light reaching the lower leaves.

To account for the remobilization of carbohydrates contained in the seed tubers (ST) during the early stages of growth, an average addition to the PA of 1 g d^{-1} for the first 20 days after plant emergence is introduced in the model (Johnson et al., 1986). Carbohydrate remobilization from stems or leaves of mature plants was not included in the model as chemical desiccation is usually applied both in field trials and in commercial production when the plant is still (partially) green. Based on this, it is assumed that there was no redistribution of carbohydrates from these organs to the tubers.

Initial values of 1, 1, 1, 0 and 1 g are assigned to the PA, LB, SB, TB and RB respectively to start the modelling process, representing the approximate weight that could be expected for the different plant organs at 50% plant emergence. The model operates at 1 m^2 surface of potato crop. Simulations start at 50% plant emergence and ends when potato plants are desiccated prior to harvest.

2.2.3. Actual yield modelling

POTATOPEST incorporates the two-damage mechanism for *P. infestans* described earlier. Stem lesions are not included in the model because of their negligible effect on yield loss compared to the leaf lesions (van Oijen, 1991a). The reduction in green area of leaves caused by *P. infestans* is proportional to the disease severity (fraction of leaf area covered by lesions) and the impact on LAI is calculated as:

$$LAI = LB \bullet SLA \bullet (1 - S) \quad (6)$$

where *S* is the disease severity recorded in the untreated plots, expressed as the leaf area in a proportion scale, with values ranging from 0 to 1 as the epidemic develops. In order to compute the second damage mechanism of *P. infestans* in potato plants (LS accelerator), and based on experimental results (van Oijen, 1991a), *S* was set to cause a proportional reduction in the lesion-free area of LB as follows:

$$LS = \begin{cases} LB \bullet (RLS + S), & LAI \le 4 \\ LB \bullet ((RLS + 0.03 \bullet (LAI - 4)/4) + S), & LAI > 4 \end{cases} \quad (7)$$

2.2.4. Model calibration and sensitivity analysis

For the attainable yield, the model was calibrated separately for the years 2001–2017 using, for each year, daily temperature, daily global solar radiation and the number of days from 50% plant emergence to desiccation as the main model inputs. Daily temperature and solar radiation data were obtained from automatic weather stations belonging to the Swedish Meteorological and Hydrological Institute (SMHI) and the Lantmet consortium weather stations network. RUE or any of the other model variables related to it (LAI, radiation intercepted) were not assessed in any of the field trials as their main goal was to test the efficacy of different fungicide mixtures and dosages in controlling late blight. Thus, RUE values were adjusted manually so that the simulated attainable yield equalled the attainable yield measured in the treated plots of the field trials, that is, RUE was set at values that resulted in matching simulated yield and measured attainable yield. The purpose of this is to use the calibrated model to produce yield estimations when the disease is present (actual yield) and to compare those estimations with the actual yield measured in the field.

A set of 100 simulations were conducted to assess the sensitivity of the model to variations in temperature and solar radiation. Each simulation was run using a thermal time of 1340 °C-day (representing the average thermal time at maturation obtained from the field trials in the calibration process) to set the end of simulation (DS=2), and temperature and PAR were the only variables left to vary from one simulation to another. In order to determine realistic ranges for temperature and solar

radiation (PAR) to be used in the sensitivity analysis, a seasonal mean temperature (mean of the daily average temperatures during the growing season of a given year) and a seasonal mean PAR (mean of the daily average PAR during the growing season of a given year) were calculated for 2001–2017. The Latin Hypercube Sampling (LHS) was then used as a sampling method to generate 100 data sequences, each sequence consisting of a pair of seasonal mean temperature and seasonal mean PAR values (Ford and Flynn, 2005). Prior to the sensitivity analysis, regression analyses between seasonal mean temperature, seasonal mean PAR and RUE were conducted to check for interdependencies between these three input variables since independent inputs are required for the percentile intervals generated by the model after the 100 simulations to be trusted (Duggan, 2019; Ford and Flynn, 2005). Since a negative correlation was found between RUE and seasonal mean PAR (RUE = -(−0.4192 *PAR) + 6.2852, r^2= 0.61), LHS was used to generate 100 sets of values for the seasonal mean temperature and seasonal mean PAR variables only, and RUE values were obtained from the equation shown above.

A second, casual sensitivity analysis was performed to assess the effect of the rate of disease growth and the time of infection on tuber yield reduction (Supplementary Fig. 2 and Supplementary Table 1). Simulations were conducted at different rates of disease growth and times of infections, at an average temperature of 16.5 °C, average PAR of 8.5 MJ d^{-1} and 94 days for the growing period.

The accuracy and precision of the model was evaluated by visually comparing the measured versus actual yields upon the 1:1 line (which represents the perfect match) in a scatterplot (Penning de Vries and Laar, 1982), and by a linear regression between the measured and actual pair values.

2.2.5. Rate of disease growth and time of infection analysis

Statistical analyses were performed to assess the impact of the disease severity and the time of infection on the yield loss using the yield loss model. The disease progress curves (DPC) for each year (1993–2017) and location were fitted using a linearized form of the logistic function defined as:

$$\ln\left(\frac{y}{1-y}\right) = \ln\left(\frac{y_0}{1-y_0}\right) + r \bullet t \tag{8}$$

where y is the disease severity (in a proportion scale, ranging from 0 to 1); $y_0$is the disease severity at the onset of the epidemic; r is the rate of disease growth (d^{-1}) and is sometimes called "apparent infection rate" (Van der Plank, 1963), and t represents the time (days after 50% plant emergence) (Madden et al., 2007).

The effect of time of plant infection (onset of epidemic) on yield reduction was characterized using a nonlinear least squares regression model:

$$\zeta(t) = \alpha \bullet e^{-\gamma \bullet t} \tag{9}$$

where $\zeta(t)$ is the loss function representing the relative yield loss, defined as the difference between attainable yield and the actual yield divided by the attainable yield; α is the maximum relative yield loss at plant emergence ($t = 0$) when the crop is infected; and γ is the tolerance of the plant to disease (d^{-1}), that is, the ability to withstand the harmful effects caused by a given pathogen when it is present in the plant (Madden et al., 2000). Time of infection (t) was estimated following Table 2. For example, if the observed disease severity in the first assessment was 0.01%, the onset of the epidemics was estimated to be 5 days before the first assessment day (see Wiik, 2014 for details).

2.3. Scenario analysis

We used POTATOPEST model to generate estimations of potential yields and yield losses (absolute and relative) caused by *P. infestans* under different climate scenarios and time periods. Temperature is decisive in disease development (Chaloner et al., 2020), and was used as the sole climate indicator to run the scenario analysis. Thus, r_t (rate of disease growth) was made dependant of temperature using a nonlinear function (similar to the one used to simulate DS) as follows:

Table 2
Estimation of the onset of the first attack of *Phytopthora infestans* based on the observed severity of the first assessment day.

% Observed disease severity	Number of days adjustment[a]
0.001%	1
> 0.001–0.0099	3
0.01–0.099	5
0.1–1.0	7
> 1.0	9

[a] Reduction of days that was applied to estimate the onset of the epidemic (first attack). See text for details

$$r_t = \begin{cases} 0, & T_d < T_{P\min} \\ \left(\frac{T_d - T_{P\min}}{T_{Popt} - T_{P\min}}\right)\left(\frac{T_{P\max} - T_d}{T_{P\max} - T_{Popt}}\right)^{\left(\frac{T_{Popt} - T_{PPmind}}{T_{P\max} - T_{P\min}}\right)}(r_{Opt}), & T_{P\min} < T_d < T_{P\max} \\ 0, & T_d > T_{P\max} \end{cases} \tag{10}$$

where, $T_{P\min}$, T_{Popt} and $T_{P\max}$ were the minimum, optimal and maximum temperatures, respectively, at which *P. infestans* develops, and correspond with values of 4.2 °C, 20.2 °C and 27.7 °C (Bebber et al., 2020; Chaloner et al., 2020). The parameter r_{Opt} represents the maximum rate of disease development at T_{Popt}, and represents a theoretical or experimentally established value, rather than the maximum value obtained in a specific experiment (Yan and Hunt, 1999). It was set to 0.43 d^{-1} as the average r value of the DPCs from the 1993–2017 field trials (see Section 3.3. *Disease progress curves and time of infection* below).

Temperature projections at regional scale (southern Sweden) were generated from an ensemble of several different regional climate models forced with several different global climate models (https://www.smhi.se/en/climate) for this scenario analysis (Table 3). These temperature projections were used to estimate rates of disease growth, which in turn were used to simulate yield losses at the different time windows and climatic scenarios.

Under two greenhouse gas emissions scenarios (RCP4.5 and RCP8.5), the increase in temperature for three-time windows (2011–2040, 2041–2070 and 2071–2100) for the growing season (June-August) were obtained from the ensemble for southern Sweden (Skåne county). This increase was calculated by comparison to a reference period (1971–2000) of observational data. The period 2001–2017, which is the period used for the calibration of POTATOPEST model in this study, was also included in the scenario analysis, and is referred to as the baseline period. All the scenario analyses were conducted at a fixed growing season of 94 days, an average PAR of 8.3 MJ m^{-2} d^{-1}, a RUE of 2.8 g MJ^{-1} and an onset of epidemics at 35 days after 50% plant emergence with an initial disease (y_0) of 0.001 (Eq. 8).

The simulation model for potato yield loss was first developed in Vensim PLE+ 8.2 (Ventana Systems, Inc.), then implemented in the R environment (R Core Team, 2021). To solve the ordinary differential equations, *deSolve* (Soetaert et al., 2010) was used, and the *FME* package (Soetaert and Petzoldt, 2010) allowed the implementation of the Latin Hypercube Sampling algorithm for the comprehensive sensitivity analysis. Function *nls* was used to fit Eq. (9).

3. Results

3.1. Attainable yield modelling

A preliminary analysis of measured attainable tuber yield (DW) showed that there was a large variation across the period 1993–2017,

Table 3
Historical (reference and baseline) temperatures measured in southern Sweden. Temperature increases projections under two emission scenarios (RPC4.5 and RPC8.5) and different time windows. Different periods refer to the following time windows: Reference (1971–2000); Baseline (2001–2017); 2025 (2011–2040); 2055 (2041–2070); 2085 (2071–2100). r_t represents the simulated rate of disease growth as a function of projected temperatures at the different time windows.

	Reference	Baseline	RCP4.5			RCP8.5		
			2025	2055	2085	2025	2055	2085
Temperature (° C)	15.4	16.6	16.7	17.5	18.0	16.8	18.0	19.7
r (d^{-1})	0.582	0.580	0.579	0.562	0.546	0.577	0.546	0.462

ranging from 700 g m^{-2} to 1600 g m^{-2}, with an average and standard deviation of 1160 and 186 g m^{-2}, respectively. Calibrated average RUE (and their standard deviations) was 2.9 (± 0.6), 2.7 (± 0.5) and 2.8 (± 0.6) g MJ^{-1} for Lilla Böslid, Mosslunda and Borgeby locations, respectively (average 2.8 g MJ^{-1}, Table 4). Seasonal mean temperature ranged between 14.7 and 18.3 °C, and seasonal mean PAR varied between 5.8 and 10 MJ m^{-2} d^{-1} (Table 4).

In general, simulated LAI values (data not shown), taken as a proxy for canopy growth, increased rapidly after plant emergence to reach a maximum value between 4 and 5.5, followed by a steady decrease until the desiccation day when the haulm was killed.

The comprehensive sensitivity analysis of the tuber yield conducted to assess the influence of meteorological input variables on the simulated attainable yields is shown in Fig. 2. Most of the 100 simulations ranged within 900–1200 g m^{-2}. Half of the simulations were clustered within a small range (1100–1200 g m^{-2}) whereas the other half varied in a wider range (900–1100 g m^{-2}). Increasing the number of simulations to 200 or even 400 did not substantially change the range of attainable yield substantially (data not shown). Overall, mean temperature and radiation had a moderate effect on the simulated attainable yield under optimal supply of water and soil nutrients.

3.2. Actual yield modelling

In general, simulated actual yields for the period 2001–2017 showed good agreement when compared to the actual yield measured in the field for the same period (Fig. 3).

The linear regression analysis showed that simulations accounted for 66.6% of this variation (r^2), with a slope of 0.76 and an intercept of 206.1 g DM m^{-2} ($p < 0.001$, n = 47, *d.f.* = 45). Standardized residuals were randomly distributed around zero over the range of simulated yield (data not shown), with a slightly higher number of positive values (low predictions) compared to negative values. There were two points (Borgeby, 2014; Mosslunda, 2015) where the difference between simulated and actual was more pronounced (with values around 2.5).

The casual sensitivity analysis carried out to assess the effect of disease growth rate and time of infection on the actual yield showed a marked response to both variables (Fig. 4).

Simulations showed that even at relatively small r, yield reductions (difference between the attainable yield and the actual yield) were substantial but, as r values increased, the magnitude of the reduction decreased (Fig. 4A and B). On the other hand, the magnitude of yield reductions remained constant as the time of infection (onset of epidemic) took place earlier in the growing season (Fig. 4C and D).

Table 4
Summary statistics of the four input variables obtained in the model calibration (2001–2017).

	Seasonal mean Temperature (°C)	Seasonal mean PAR (MJ m^{-2} d^{-1})	RUE (g MJ^{-1})	Growing Period (d)
Average	16.57	8.30	2.80	94.21
Standard deviation	0.79	1.04	0.56	6.74
Maximum	18.27	9.95	4.50	107.00
Minimum	14.73	5.75	1.85	74.00
Quartiles				
1st (25%)	16.05	8.15	2.45	90.00
Median	16.54	8.50	2.70	95.00
3rd (75%)	17.14	8.83	2.98	99.00
Skewness	0.10	-0.84	0.96	-0.51
Kurtosis	0.11	0.28	0.88	0.51

3.3. Disease progress curves and time of infection

All DPCs recorded in the untreated plots (period 1993–2017) reached 100% severity, with variations in the start of the infection and in the slope of the curve. The logistic model fitted most of the DPCs well, with coefficients of determination (r^2) above 0.9 in 88% of the total DPCs, and the remaining cases with values above 0.8 (except one single case, with a r^2 of 0.73). The rate of disease growth parameter (r) ranged from 0.17 d^{-1} to 0.77 d^{-1}, with an average and standard deviation of 0.43

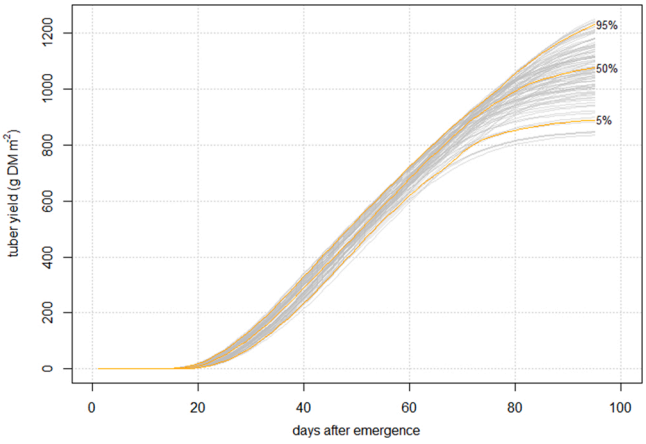

Fig. 2. Simulated tuber attainable yield. Each line represents one simulation out of 100 with a specific pair of temperature and PAR values varying within the ranges set in Table 4, with 94 days as a simulation time and RUE dependent on PAR. Percentages represent percentile intervals so that 50% represents the median of all the simulations. Yield units are in grams tuber dry matter per square meter.

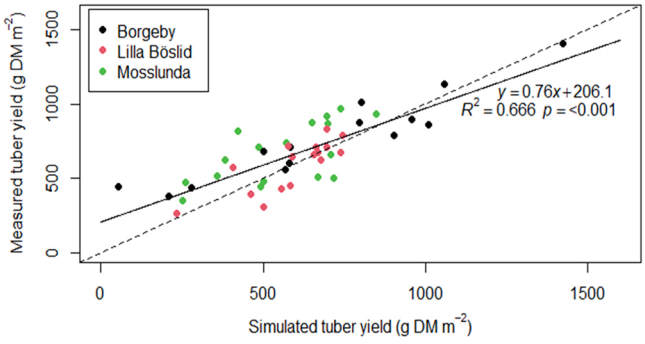

Fig. 3. Comparison of the simulated and the measured tuber yield (g DM m^{-2}) for the period 2001–2017 in untreated plots (actual yield). Each dot represents one year at the specified location (see legend). Dashed line represents the 1:1 line. Solid line represents the regression line.

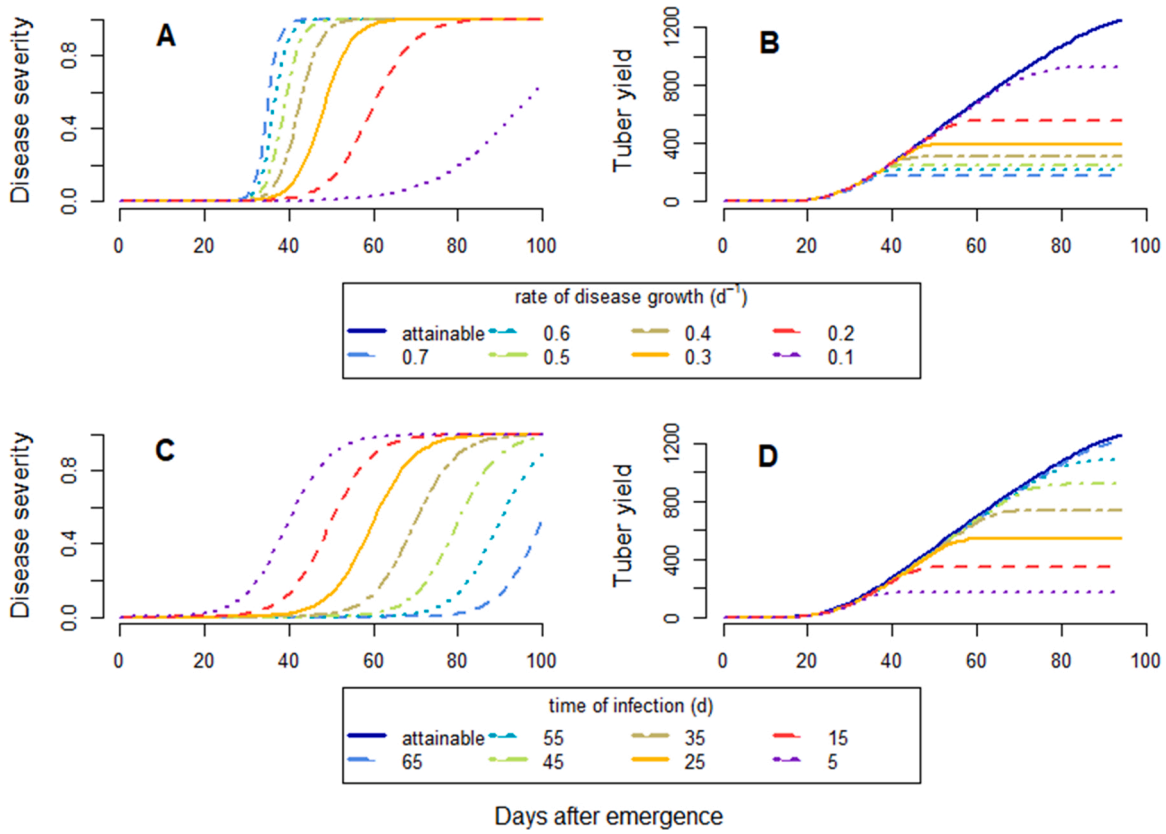

Fig. 4. Simulations showing a varying rate of disease growth, time of infection and their associated yields. Fig. 4A represents simulated DPCs at different rates of disease growth (but all starting at 25 days after plant emergence), while Fig. 4C represents simulated DPCs at different starting days of the epidemic (but all with the same rate of disease growth of 0.2 d^{-1}). Fig. 4B and D show the simulated yields associated to the different DPCs in 4A and 4C, respectively.

d^{-1} and 0.16 d^{-1}, respectively. There was one single extreme case with a *r* value of 0.95 d^{-1}, corresponding with the epidemic of 2006. In this year and location, disease severity recorded at the second assessment day was nearly 3%, followed by a 99% severity in the next assessment, after only 6 days.

There was a large variation in the time of infection, with epidemics starting as soon as the plant emerged and others as late as 80 days after plant emergence. For example, the epidemic in 2014 in Borgeby was estimated to start two days before the day when 50% plants emergence was recorded, meaning that the plants were infected by the pathogen at emergence. The impact of the time of infection on yield loss decreased exponentially with the delay in the time of infection (Fig. 5), although there was a high variability. The negative exponential equation provided a reasonable fit, with an α of 0.73 and a γ of 0.015 d^{-1}.

3.4. Scenario analysis

Model estimates showed a decrease of attainable yields (Fig. 6) as projected temperatures increase towards the end of the century for both emissions scenarios (Table 3), although this decrease in attainable yield was more pronounced for the more drastic scenario RPC8.5. The increase in temperature accelerates the phenological development rate of the potato crop, with an earlier maturation and onset of natural senescence and therefore less time for the plant to build up canopy and photoassimilates production.

Yield losses (absolute and relative) caused by *P. infestans* (when fungicides are not applied) also decreased as the projected rise in temperature towards the end of the century makes *r* decrease from its optimum following the nonlinear distribution function (Table 3). This decrease in yield loss is again more pronounced at later time windows when temperature projections are higher and for the more drastic emission scenario. Despite the reduction in projected attainable yields, projected actual yields (attainable yields minus losses) tended to increase. This can be explained by the better ability of the potato plant to tolerate higher temperatures compared to *P. infestans*, which causes projected losses to be less pronounced as time progresses.

4. Discussion

This study presents a simulation model able to provide estimations of

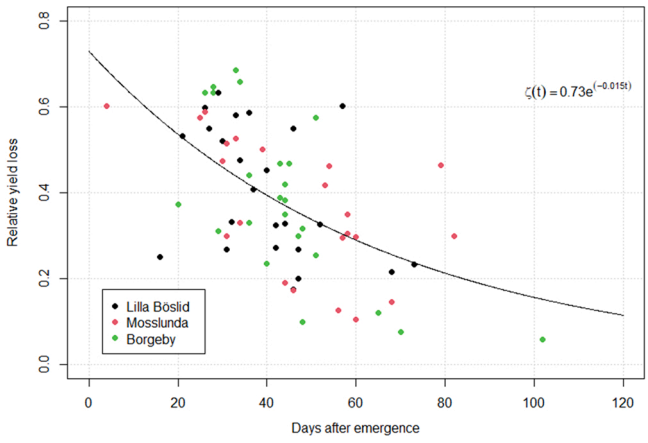

Fig. 5. Tuber yield loss as a function of the time of infection by *P. infestans* for the period 1993–2017 in potato cultivar Bintje. Points represent the different locations and years. Solid curve represents the predicted values from the loss function (Eq. 9).

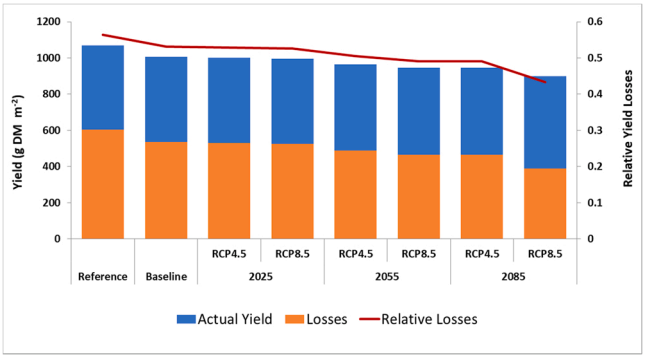

Fig. 6. Actual yield (with late blight), yield loss caused by *P. infestans* and relative yield loss (yield loss divided by the attainable yield, in relative units) estimations for two emission scenarios and different time windows Reference (1971–2000); Baseline (2001–2017); 2025 (2011–2040); 2055 (2041–2070); 2085 (2071–2100). The height of each column (actual yield + losses) represents the attainable yield.

yield loss in potato crop caused by *P. infestans*. The model allows for the quantification of the effects of some of the epidemiological traits for late blight commonly determined at field scale such as the rate of disease growth and the start of the epidemics on yield reduction and exhibits the potential of any disease control measure aimed at reducing these factors to reduce yield losses.

Radiation use efficiency in potato crop tends to be higher than in other crops due to the low energy content of the starch of the tubers (Murchie and Reynolds, 2013). Estimates of RUE for potato crops grown in optimal conditions (attainable yield) have been reported to vary from 1.81 to 3.17 g MJ^{-1} in The Netherlands (van Oijen, 1991b), 3.4 g MJ^{-1} in Finland (Kaukoranta, 1996), 2.0–4.0 g MJ^{-1} in Denmark (Zhou et al., 2017), 3.2 g MJ^{-1} in Israel (Waggoner and Berger, 1987) and 3.5–3.9 g MJ^{-1} in the United Kingdom (Jefferies and Mackerron, 1989). Except for one single extreme value of 4.5 g MJ^{-1} (Table 4), the variation in calibrated RUE values obtained during the attainable yield modelling lay within the range reported in the literature obtained from empirical studies under optimal agronomic conditions, indicating that the model structure performs well. The negative relationship between RUE and PAR detected as a preliminary step before conducting the sensitivity analysis has been calculated elsewhere (Wolf and Van Oijen, 2003), supporting the inclusion of RUE as a dependent variable of PAR and therefore allowing the exploration of the effect of only the variables temperatures and PAR on the attainable yield in the sensitivity analysis (Fig. 2). Seasonal mean temperature varied by nearly 4 °C and PAR more than 4 MJ m^{-2} d^{-1} during the calibration years (2001–2017), pointing out the range of average temperatures and solar radiation that can be expected in a short-term climatic future and the associated potential yield (Table 4, Fig. 2).

The large variability in both the attainable and actual tuber yield observed in the field trials is largely due to the interaction of the meteorological variables promoting the spread of the pathogen and shifts in the local pathogen population itself, with some strains more aggressive than others. Disease progress curves can be used to describe this interaction, with years showing a delayed and less steep DPC and other years with very steep curves starting early in the growing season. The POTATOPEST model incorporates the effect of the pathogen on yield in two different ways; first by reducing the green leaf area in a proportional way to the development of the DPC, and then by increasing the natural leaf senescence, also proportional to the DPC. The relatively small differences between simulated actual yield and the observed values (Fig. 3) indicate that the model satisfactorily incorporates these two damage mechanisms and that they explain a large proportion of the variation in yield reduction. This close match between observed and simulated actual yield in untreated plots is a robust criterion for the validity of the POTATOPEST model (Rykiel, 1996).

However, there may be room for further improvement of the model if other damage mechanisms for *P. infestans* are documented and parameterized. Apart from the two mechanisms already described in this study, there are two other injury mechanisms characteristic of foliar diseases. The first of these mechanisms is the formation of virtual lesions adjacent to the visual lesions, where the photosynthetic activity is diminished despite the fact that the tissue remains symptom-free at naked eye (Bastiaans, 1991). To the best of our knowledge, no such effect has been documented for *P. infestans* in potato. Should this damage mechanism be confirmed and experimentally quantified, its effect could be introduced in POTATOPEST as a reduction in LAI (and therefore a reduction in the radiation intercepted by the crop canopy) additional to the effects currently quantified in the model by the formation and development of visual leaf lesions. The second potential mechanism affecting yield reduction is the diversion of the host plant's photoassimilates to the infected sites for the development and dissemination of the pathogen (Hohl and Stössel, 1976; Hohl and Suter, 1976). Again, no quantification or estimates of the fraction of the host's assimilates diverted to the pathogen development has been reported to our knowledge. In very susceptible potato cultivars like Bintje these two processes may not be significant in terms of their contribution to yield reduction as the other two processes parameterized in the model already account for a large variation in yield loss. However, in more resistant cultivars, these mechanisms may explain a greater variation in yield reduction and warrants future research.

In addition, *P. infestans* can also infect potato tubers during or after harvest by the spores produced in the foliage, leading to important reductions in yield quality (Guenthner et al., 2001). Recently, injuries of the harvestable organs have been proposed as an additional damage mechanism (Savary and Willocquet, 2020) to be added to the already documented damage mechanisms that should be considered in future yield loss assessments. However, modelling of this specific damage mechanism has been sparsely studied, with inconsistent results (Nyankanga et al., 2011; Wiik, 2014). Among others, epidemiological traits such as the level and duration of foliage blight (and therefore inoculum density) have been reported to influence the occurrence of tuber blight (Nyankanga et al., 2011). Epidemiological H-L-I-R models (Healthy, Latent, Infectious, Removed) are the equivalent to S-E-I-R (Susceptible, Exposed, Infectious, Removed) models in human and animal epidemiology (Diekmann and Heesterbeek, 2000), and describe the dynamics of the infectious process at individual level (Madden et al., 2007). Therefore, coupling POTATOPEST with H-L-I-R epidemiological dynamic models would be highly desirable, in a similar way as previous works did to characterise *P. infestans* dispersion and risk of infection at landscape level (Skelsey et al., 2010, 2009b), and it would allow a better characterisation of tuber blight and post-harvest yield loss estimation.

Simulated tuber yields in POTATOPEST model are very sensitive to changes in both rate of disease growth and time of the start of the epidemic; small changes in any of these parameters entail a considerable effect on yield reduction and therefore, from a practical disease control, any action that delays time of infection and reduces rate of disease growth can have significant reductions in yield losses. To our knowledge, no attempt to characterize potato yield loss as a function of the time of infection by *P. infestans* has been done before. The parameters (α, γ) from the loss function (Eq. 9) are usually considered to represent a measure of the tolerance of a plant species or cultivar to a disease. Mathematically, γ represents the decay rate (slope) of the yield loss caused by the pathogen with the time of onset of the epidemic. This means that at larger γ, yield losses diminish faster as the onset of the epidemic occurs later, whereas at smaller γ the reduction in yield remains large (Madden et al., 2000). In our study, the estimation of the tolerance level in Bintje (α and γ parameters) was based on the data from 25 years, during which the local pathogen population is likely to have changed from being dominated by a few clonal strains to a highly variable sexual population (Yuen and Andersson, 2013). Therefore, this

mathematical evaluation of the tolerance of Bintje can be considered as a good proxy of the aggressiveness of the local populations of *P. infestans*. Breeding programmes where tolerance to *P. infestans* is implemented may have a large potential to improve current plant protection strategies by breaking the co-evolutionary cycle between the crop resistance and the adaptation of the pathogen (Masini et al., 2019; Rausher, 2001). Knowledge of the population structure and adaptation in pathogens is important when evaluating disease tolerance and yield loss in field trials, which is evident from the recent rapid population turnover in *P. infestans* (Wu et al., 2020; Yuen and Andersson, 2013) and in other pathogens (Berlin et al., 2012; Karlsson et al., 2017).

The estimated values for r agree with other studies. For example, Hannukkala et al. (2007) found an average r of 0.45 d^{-1} in field trials in Finland with cultivar Bintje. A possible explanation for the early outbreaks, like the one recorded in 2014 in Borgeby, is the presence of oospores in the soil that germinated with the emergence of the first plants, allowing a very early onset of the disease (Hannukkala et al., 2007; Lehsten et al., 2017; Wiik, 2014). Several studies have confirmed the occurrence of oospores in Sweden due to the presence of both mating types of *P. infestans* (Andersson et al., 1998; Sjöholm et al., 2013).

In our scenario analysis, increases in the average temperature led to moderate reductions in attainable yield. This analysis is limited by two factors; 1) POTATOPEST model does not consider the stimulating effect of atmospheric CO_2 on crop growth and tuber production. Several studies on potato production and climate change (elevated atmospheric CO_2 and temperatures) suggested that elevated CO_2 may offset the detrimental effects of high temperatures on crop development and yields, although there are contradicting results (Jennings et al., 2020; Raymundo et al., 2018), and 2) our analysis considered a fixed average growing season of 94 days (equivalent to 1340 °C-day to reach maturation). Longer growing seasons with earlier planting dates have been proposed as a strategy to compensate for the detrimental effects of higher temperatures on the phenological development of potato crop in future climate scenarios (Naz et al., 2022; Skelsey et al., 2016), provided that crops are grown in nonlimiting conditions with optimal water and nutrients supply. On the other hand, our scenario analysis suggests that the rise in temperatures may push *P. infestans* far from its optimum development and therefore decrease the rate of disease growth and subsequent yield losses. However, this analysis is limited by two factors; 1) the large uncertainties in projected relative humidity (RH) towards the end of the century diminishes the value of this parameter to determine reliable disease growth estimates. In fact, a recent study suggests that temperature alone was sufficient to model fungal and oomycete activity satisfactorily without using RH (Chaloner et al., 2021), and 2) *P. infestans* can adapt to increasing temperatures in laboratory conditions (Wu et al., 2020; Yang et al., 2016), although pathogen adaptation in field conditions is slow compared to the increase in temperature expected in the ongoing climate change (Bebber et al., 2013).

Despite the limitations of this scenario analysis, the approach is useful to inform more detailed studies and to guide potato production for adaptation to climate change. Traditionally, early planting in higher latitudes is seen as a way to adapt to warming growing season, thus maximizing crop production. The ongoing increase in temperatures is likely to reinforce this trend. However, the results of the scenario analysis suggest that maintaining current planting dates with late harvests may alleviate the impact of late blight as a consequence of the narrower tolerance to higher temperatures of the pathogen compared to the plant. Starting the growing season earlier in the year due to milder springs might favour the disease development and the subsequent decrease in tuber yield, therefore requiring prolonged fungicide applications to maintain high yields.

In conclusion, the POTATOPEST model presented here allows the assessment of the damage caused by *P. infestans* in potato crops. The model produced reasonable estimates of tuber yield and its reduction caused by *P. infestans* based on relatively small number of agronomical input variables. The model allowed the assessment of the role that the rate of disease growth and the time of the start of the infection play in yield reduction. In addition, the effect of rising temperatures was also evaluated, suggesting that *P. infestans* might cause less yield loss as the pathogen deviates from its optimum development. The model can be adapted to other cultivars and regions, especially at high latitudes. Late blight is currently controlled mainly by repeated fungicide application. POTATOPEST could be used to analyse productivity, resistance and tolerance of new potato cultivars in the continuous quest of the scientific and growers' community to reduce the use of fungicides due to their negative effects on the environment. In this context, the predictive model output may be used by agricultural advisors as part of IPM programs. As a mechanistic model, POTATOPEST allows the incorporation of other pests and diseases in future studies. In this way, it is possible to use the model to analyse a specific (present or future) combination of multiple pests and diseases characteristic of a given region of interest, and to evaluate improved and efficient management options.

CRediT authorship contribution statement

José González-Jiménez: Conceptualization, Formal analysis, Investigation, Methodology, Project administration, Resources, Software, Validation, Visualization, Writing – original draft. **Björn Andersson:** Conceptualization, Formal analysis, Funding acquisition, Investigation, Methodology, Project administration, Resources, Software, Supervision, Validation, Visualization, Writing – original draft. **Lars Wiik:** Data curation, Investigation, Supervision, Validation, Writing – review & editing. **Jiasui Zhan:** Conceptualization, Formal analysis, Funding acquisition, Investigation, Methodology, Project administration, Resources, Software, Supervision, Validation, Visualization, Writing – original draft.

Declaration of Competing Interest

The authors declare that they have no known competing financial interests or personal relationships that could have appeared to influence the work reported in this paper.

Data Availability

Data will be made available on request.

Acknowledgments

Salary and research support for J. González-Jiménez was provided by national funds through SLU Uppsala, Sweden. We would like to thank the participants of the EU-funded EIP project titled *Improved IPM in potato cultivation* for their support and advice in the development and implementation of the model, and to Anna Berlin for valuable comments reviwing an early version of this manuscript. The authors would also like to thank three annonymous reviewers and the managing editor for their comments and corrections, which helped to improve the whole document.

Appendix A. Supporting information

Supplementary data associated with this article can be found in the online version at doi:10.1016/j.fcr.2023.108977.

References

Andersson, B., Sandström, M., Strömberg, A., 1998. Indications of soil borne inoculum of *Phytophthora infestans*. Potato Res. 41, 305–310. https://doi.org/10.1007/BF02358962.

Bangemann, L.-W., Sieling, K., Kage, H., 2014. The effect of nitrogen and late blight on crop growth, solar radiation interception and yield of two potato cultivars. F. Crop. Res. 155, 56–66. https://doi.org/10.1016/j.fcr.2013.09.022.

Bastiaans, L., 1991. Ratio between virtual and visual lesion size as a measure to describe reduction in leaf photosynthesis of rice due to leaf blast. Phytopathology 81, 611–615.
Bebber, D.P., Ramotowski, M.A.T., Gurr, S.J., 2013. Crop pests and pathogens move polewards in a warming world. Nat. Clim. Chang. 3, 985–988. https://doi.org/10.1038/nclimate1990.
Bebber, D.P., Chaloner, T.M., Gurr, S.J., 2020. Fungal and Oomycete cardinal temperatures (the Togashi dataset). Dryad, Dataset.
Berlin, A., Djurle, A., Samils, B., Yuen, J., 2012. Genetic variation in Puccinia graminis collected from oats, rye, and barberry. Phytopathology® 102, 1006–1012. https://doi.org/10.1094/PHYTO-03-12-0041-R.
Boote, K.J., Jones, J.W., Mishoe, J.W., Berger, R.D., 1983. Coupling pests to crop growth simulators to predict yield reductions. Phytopathology 73, 1581–1587.
Bourke, P.M.A., 1955. The Forecasting from Weather Data of Potato Blight and Other Plant Diseases and Pests: First Report of the Working Group on Weather and Plant Pathology Problems, of the Commission for Agricultural Meteorology, Technical note - World Meteorological Organization. Secretariat of the World Meteorological Organization.
Burdon, J.J., Barrett, L.G., Yang, L.-N., He, D.-C., Zhan, J., 2019. Maximizing world food production through disease control. Bioscience 70, 126–128. https://doi.org/10.1093/biosci/biz149.
Chaloner, T.M., Gurr, S.J., Bebber, D.P., 2020. Geometry and evolution of the ecological niche in plant-associated microbes. Nat. Commun. 11, 2955. https://doi.org/10.1038/s41467-020-16778-5.
Chaloner, T.M., Gurr, S.J., Bebber, D.P., 2021. Plant pathogen infection risk tracks global crop yields under climate change. Nat. Clim. Chang. 11, 710–715. https://doi.org/10.1038/s41558-021-01104-8.
Davis, K.F., Gephart, J.A., Emery, K.A., Leach, A.M., Galloway, J.N., D'Odorico, P., 2016. Meeting future food demand with current agricultural resources. Glob. Environ. Chang. 39, 125–132. https://doi.org/10.1016/j.gloenvcha.2016.05.004.
Devaux, A., Goffart, J.-P., Petsakos, A., Kromann, P., Gatto, M., Okello, J., Suarez, V., Hareau, G., 2020. Global food security, contributions from sustainable potato agri-food systems. In: Campos, H., Ortiz, O. (Eds.), The Potato Crop: Its Agricultural, Nutritional and Social Contribution to Humankind. Springer International Publishing, Cham, pp. 3–35. https://doi.org/10.1007/978-3-030-28683-5_1.
Diekmann, O., Heesterbeek, J.A.P., 2000. Mathematical epidemiology of infectious diseases: model building, analysis and interpretation. Wiley Series in Mathematical and Computational Biology. John Wiley and Sons,, United States.
Donatelli, M., Magarey, R.D., Bregaglio, S., Willocquet, L., Whish, J.P.M., Savary, S., 2017. Modelling the impacts of pests and diseases on agricultural systems. Agric. Syst. 155, 213–224. https://doi.org/10.1016/j.agsy.2017.01.019.
Duggan, J., 2019. Using R libraries to facilitate sensitivity analysis and to calibrate system dynamics models. Syst. Dyn. Rev. 35, 255–282. https://doi.org/10.1002/sdr.1638.
Esker, P.D., Savary, S., McRoberts, N., 2012. Crop loss analysis and global food supply: focusing now on required harvests. CAB Rev. 7, 1–14.
Ford, A., Flynn, H., 2005. Statistical screening of system dynamics models. Syst. Dyn. Rev. 21, 273–303.
Gaunt, R.E., 1995. The relationship between plant disease severity and yield. Annu. Rev. Phytopathol. 33, 119–144. https://doi.org/10.1146/annurev.py.33.090195.001003.
Godfray, H.C.J., Beddington, J.R., Crute, I.R., Haddad, L., Lawrence, D., Muir, J.F., Pretty, J., Robinson, S., Thomas, S.M., Toulmin, C., 2010. Food security: the challenge of feeding 9 billion people. Science 80-. (327), 812–818. https://doi.org/10.1126/science.1185383.
Guenthner, J.F., Michael, K.C., Nolte, P., 2001. The economic impact of potato late blight on US growers. Potato Res 44, 121–125. https://doi.org/10.1007/BF02410098.
Hannukkala, A.O., Kaukoranta, T., Lehtinen, A., Rahkonen, A., 2007. Late-blight epidemics on potato in Finland, 1933–2002; increased and earlier occurrence of epidemics associated with climate change and lack of rotation. Plant Pathol. 56, 167–176. https://doi.org/10.1111/j.1365-3059.2006.01451.x.
Haverkort, A.J., Bicamumpaka, M., 1986. Correlation between intercepted radiation and yield of potato crops infested by *Phytophthora infestans* in central Africa. Neth. J. Plant Pathol. 92, 239–247.
He, D.-C., Burdon, J.J., Xie, L., Zhan, J., 2021a. Triple bottom-line consideration of sustainable plant disease management: from economic, sociological and ecological perspectives. J. Integr. Agric. 20, 2581–2591. https://doi.org/10.1016/S2095-3119(21)63627-4.
He, D.-C., He, M.-H., Amalin, D.M., Liu, W., Alvindia, D.G., Zhan, J., 2021b. Biological control of plant diseases: an evolutionary and eco-economic consideration. Pathogens 10. https://doi.org/10.3390/pathogens10101311.
Hohl, H.R., Stössel, P., 1976. Host–parasite interfaces in a resistant and a susceptible cultivar of *Solanum tuberosum* inoculated with *Phytophthora infestans*: tuber tissue. Can. J. Bot. 54, 900–912. https://doi.org/10.1139/b76-094.
Hohl, H.R., Suter, E., 1976. Host–parasite interfaces in a resistant and a susceptible cultivar of *Solanum tuberosum* inoculated with *Phytophthora infestans*: leaf tissue. Can. J. Bot. 54, 1956–1970. https://doi.org/10.1139/b76-209.
IPBES, 2019. Summary for Policymakers of the Global Assessment Report on Biodiversity and Ecosystem Services of the Intergovernmental Science-Policy Platform on Biodiversity and Ecosystem Services. IPBES Secretariat, Bonn, Germany.
Isard, S.A., Russo, J.M., Magarey, R.D., Golod, J., VanKirk, J.R., 2015. Integrated pest information platform for extension and education (iPiPE): progress through sharing. J. Integr. Pest Manag. 6. https://doi.org/10.1093/jipm/pmv013.
Jefferies, R.A., Mackerron, D.K.L., 1989. Radiation interception and growth of irrigated and droughted potato (*Solanum tuberosum*). F. Crop. Res. 22, 101–112. https://doi.org/10.1016/0378-4290(89)90061-0.
Jennings, S.A., Koehler, A.-K., Nicklin, K.J., Deva, C., Sait, S.M., Challinor, A.J., 2020. Global potato yields increase under climate change with adaptation and CO_2 fertilisation. Front. Sustain. Food Syst. 4, 248. https://doi.org/10.3389/fsufs.2020.519324.
Johnson, K.B., 1992. Evaluation of a mechanistic model that describes potato crop losses caused by multiple pests. Phytopathology 82, 363–369.
Johnson, K.B., Johnson, S.B., Teng, P.S., 1986. Development of a simple potato growth model for use in crop-pest management. Agric. Syst. 19, 189–209. https://doi.org/10.1016/0308-521X(86)90052-1.
Jones, J.W., Antle, J.M., Basso, B., Boote, K.J., Conant, R.T., Foster, I., Godfray, H.C.J., Herrero, M., Howitt, R.E., Janssen, S., Keating, B.A., Munoz-Carpena, R., Porter, C. H., Rosenzweig, C., Wheeler, T.R., 2017. Brief history of agricultural systems modeling. Agric. Syst. 155, 240–254. https://doi.org/10.1016/j.agsy.2016.05.014.
Juroszek, P., von Tiedemann, A., 2015. Linking plant disease models to climate change scenarios to project future risks of crop diseases: a review. J. Plant Dis. Prot. 122, 3–15. https://doi.org/10.1007/BF03356525.
Kabat, P., Marshall, B., Broek, B.J. van den, Vos, J., Keulen, H. van, 1995. Modelling and parameterization of the soil-plant-atmosphere system; a comparison of potato growth models. Wageningen Pers, 141, Agronomie,.
Karlsson, I., Friberg, H., Kolseth, A.-K., Steinberg, C., Persson, P., 2017. Agricultural factors affecting *Fusarium* communities in wheat kernels. Int. J. Food Microbiol 252, 53–60. https://doi.org/10.1016/j.ijfoodmicro.2017.04.011.
Kaukoranta, T., 1996. Impact of global warming on potato late blight: risk, yield loss and control. Agric. Food Sci. 5, 311–327. https://doi.org/10.23986/afsci.72749.
Kooman, P.L., Fahem, M., Tegera, P., Haverkort, A.J., 1996. Effects of climate on different potato genotypes 2. Dry matter allocation and duration of the growth cycle. Eur. J. Agron. 5, 207–217. https://doi.org/10.1016/S1161-0301(96)02032-1.
Leesutthiphonchai, W., Vu, A.L., Ah-Fong, A.M.V., Judelson, H.S., 2018. How does Phytophthora infestans evade control efforts? Modern insight into the late bight disease. Phytopathology® 108, 916–924. https://doi.org/10.1094/PHYTO-04-18-0130-IA.
Lehsten, V., Wiik, L., Hannukkala, A., Andreasson, E., Chen, D., Ou, T., Liljeroth, E., Lankinen, Å., Grenville-Briggs, L., 2017. Earlier occurrence and increased explanatory power of climate for the first incidence of potato late blight caused by *Phytophthora infestans* in Fennoscandia. PLoS One 12, 1–21. https://doi.org/10.1371/journal.pone.0177580.
Madden, L.V., Hughes, G., Irwin, M.E., 2000. Coupling disease-progress-curve and time-of-infection functions for predicting yield loss of crops. Phytopathology 90, 788–800. https://doi.org/10.1094/PHYTO.2000.90.8.788.
Madden, L.V., Hughes, G., van den Bosch, F., 2007. The study of plant disease epidemics. The American Phytopathological Society, St. Paul, MN. https://doi.org/10.1094/9780890545058.
Magarey, R.D., Travis, J.W., Russo, J.M., Seem, R.C., Magarey, P.A., 2002. Decision support systems: quenching the thirst. Plant Dis. 86, 4–14. https://doi.org/10.1094/PDIS.2002.86.1.4.
Masini, L., Grenville-Briggs, L.J., Andreasson, E., Råberg, L., Lankinen, Å., 2019. Tolerance and overcompensation to infection by *Phytophthora infestans* in the wild perennial climber *Solanum dulcamara*. Ecol. Evol. 9, 4557–4567. https://doi.org/10.1002/ece3.5057.
Monteith, J.L., 1977. Climate and the efficiency of crop production in Britain. Philos. Trans. R. Soc. Lond. B, Biol. Sci. 281, 277–294. https://doi.org/10.1098/rstb.1977.0140.
Monteith, J.L., Unsworth, M.H., 2013. Chapter 8 - Microclimatology of radiation: (iii) Interception by plant canopies and animal coats. In: Monteith, J.L., Unsworth, M.H. (Eds.), Principles of Environmental Physics, fourth ed. Academic Press, Boston, pp. 111–133. https://doi.org/10.1016/B978-0-12-386910-4.00008-1.
Murchie, E., Reynolds, M., 2013. Crop radiation capture and use efficiency. In: Christou, P., Savin, R., Costa-Pierce, B.A., Misztal, I., Whitelaw, C.B.A. (Eds.), Sustainable Food Production. Springer, New York, New York, NY, pp. 591–614. https://doi.org/10.1007/978-1-4614-5797-8_171.
Naz, S., Ahmad, S., Abbas, G., Fatima, Z., Hussain, S., Ahmed, M., Khan, M.A., Khan, A., Fahad, S., Nasim, W., Ercisli, S., Wilkerson, C.J., Hoogenboom, G., 2022. Modeling the impact of climate warming on potato phenology. Eur. J. Agron. 132, 126404 https://doi.org/10.1016/j.eja.2021.126404.
Nyankanga, R.O., Olanya, O.M., Ojiambo, P.S., Wien, H.C., Honeycutt, C.W., Kirk, W.W., 2011. Validation of tuber blight (*Phytophthora infestans*) prediction model. Crop Prot. 30, 547–553. https://doi.org/10.1016/j.cropro.2010.11.019.
van Oijen, M., 1991a. Leaf area dynamics of potato cultivars infected by *Phytophthora infestans*. Neth. J. Plant Pathol. 97, 345–354. https://doi.org/10.1007/BF03041383.
van Oijen, M., 1991b. Light use efficiencies of potato cultivars with late blight (*Phytophthora infestans*). Potato Res. 34, 123–132. https://doi.org/10.1007/BF02358033.
van Oijen, M., 1992. Evaluation of breeding strategies for resistance and tolerance to late blight in potato by means of simulation. Neth. J. Plant Pathol. 98, 3–11. https://doi.org/10.1007/BF01998073.
Penning de Vries, F.W.T., Laar, H.H. van, 1982. Simulation of plant growth and crop production, Simulation monographs. Pudoc, 140, Laboratorium voor Theoretische Productie Ecologie en Agronomie,.
Pulatov, B., Linderson, M.-L., Hall, K., Jönsson, A.M., 2015. Modeling climate change impact on potato crop phenology, and risk of frost damage and heat stress in northern Europe. Agric. Meteorol. 214–215, 281–292. https://doi.org/10.1016/j.agrformet.2015.08.266.
R Core Team, 2021. R: A language and environment for statistical computing. R Foundation for Statistical Computing, Vienna, Austria. https://www.R-project.org/.
Rabbinge, R., 1993. The ecological background of food production. In: Crop Protection and Sustainable Agriculture. John Wiley & Sons, Chicester, pp. 2–29.

Rakotonindraina, T., Chauvin, J.-É., Pellé, R., Faivre, R., Chatot, C., Savary, S., Aubertot, J.-N., 2012. Modeling of yield losses caused by potato late blight on eight cultivars with different levels of resistance to Phytophthora infestans. Plant Dis. 96, 935–942. https://doi.org/10.1094/PDIS-09-11-0752.

Rausher, M.D., 2001. Co-evolution and plant resistance to natural enemies. Nature 411, 857–864. https://doi.org/10.1038/35081193.

Raymundo, R., Asseng, S., Cammarano, D., Quiroz, R., 2014. Potato, sweet potato, and yam models for climate change: a review. F. Crop. Res. 166, 173–185. https://doi.org/10.1016/j.fcr.2014.06.017.

Raymundo, R., Asseng, S., Robertson, R., Petsakos, A., Hoogenboom, G., Quiroz, R., Hareau, G., Wolf, J., 2018. Climate change impact on global potato production. Eur. J. Agron. 100, 87–98. https://doi.org/10.1016/j.eja.2017.11.008.

Rossing, W.A.H., Oijen, M. van, Werf, W. van der, Bastiaans, L., Rabbinge, R., 1992. Modelling the effects of foliar pests and pathogens on light interception, photosynthesis, growth rate and yield of field crops., in: Ayres, P.G. (Ed.), Pests and Pathogens, Plant Responses to Foliar Attack. BIOS Scient. Publ, 140, Laboratorium voor Theoretische Productie Ecologie en Agronomie, pp. 161–180.

Rouse, D.I., 1988. Use of crop growth-models to predict the effects of disease. Annu. Rev. Phytopathol. 26, 183–201. https://doi.org/10.1146/annurev.py.26.090188.001151.

Rykiel, E.J., 1996. Testing ecological models: the meaning of validation. Ecol. Modell. 90, 229–244. https://doi.org/10.1016/0304-3800(95)00152-2.

Savary, S., Willocquet, L., 2014. Simulation modeling in botanical epidemiology and crop loss analysis. Plant Heal. Instr. https://doi.org/10.1094/phi-a-2014-0314-01.

Savary, S., Willocquet, L., 2020. Modeling the impact of crop diseases on global food security. Annu. Rev. Phytopathol. 58, 313–341. https://doi.org/10.1146/annurev-phyto-010820-012856.

Savary, S., Nelson, A.D., Djurle, A., Esker, P.D., Sparks, A., Amorim, L., Bergamin Filho, A., Caffi, T., Castilla, N., Garrett, K., McRoberts, N., Rossi, V., Yuen, J., Willocquet, L., 2018. Concepts, approaches, and avenues for modelling crop health and crop losses. Eur. J. Agron. 100, 4–18. https://doi.org/10.1016/j.eja.2018.04.003.

Savary, S., Willocquet, L., Pethybridge, S.J., Esker, P., McRoberts, N., Nelson, A., 2019. The global burden of pathogens and pests on major food crops. Nat. Ecol. Evol. 3, 430–439. https://doi.org/10.1038/s41559-018-0793-y.

Sjöholm, L., Andersson, B., Högberg, N., Widmark, A.-K., Yuen, J., 2013. Genotypic diversity and migration patterns of *Phytophthora infestans* in the Nordic countries. Fungal Biol. 117, 722–730. https://doi.org/10.1016/j.funbio.2013.08.002.

Skelsey, P., Kessel, G.J.T., Rossing, W.A.H., van der Werf, W., 2009a. Parameterization and evaluation of a spatiotemporal model of the potato late blight pathosystem. Phytopathology® 99, 290–300. https://doi.org/10.1094/PHYTO-99-3-0290.

Skelsey, P., Rossing, W.A.H., Kessel, G.J.T., van der Werf, W., 2009b. Scenario approach for assessing the utility of dispersal information in decision support for aerially spread plant pathogens, applied to Phytophthora infestans. Phytopathology® 99, 887–895. https://doi.org/10.1094/PHYTO-99-7-0887.

Skelsey, P., Rossing, W.A.H., Kessel, G.J.T., van der Werf, W., 2010. Invasion of Phytophthora infestans at the landscape level: how do spatial scale and weather modulate the consequences of spatial heterogeneity in host resistance? Phytopathology® 100, 1146–1161. https://doi.org/10.1094/PHYTO-06-09-0148.

Skelsey, P., Cooke, D.E.L., Lynott, J.S., Lees, A.K., 2016. Crop connectivity under climate change: future environmental and geographic risks of potato late blight in Scotland. Glob. Chang. Biol. 22, 3724–3738. https://doi.org/10.1111/gcb.13368.

Soetaert, K., Petzoldt, T., 2010. Inverse modelling, sensitivity and Monte Carlo analysis in R using package FME. J. Stat. Softw., Artic. 33, 1–28. https://doi.org/10.18637/jss.v033.i03.

Soetaert, K., Petzoldt, T., Setzer, R.W., 2010. Solving differential equations in R: package deSolve. J. Stat. Softw., Artic. 33, 1–25. https://doi.org/10.18637/jss.v033.i09.

Sterman, J.D., 2000. Business Dynamics: Systems Thinking and Modeling for A Complex World. Irwin/McGraw-Hill, Boston.

Streck, N.A., de Paula, F.L.M., Bisognin, D.A., Heldwein, A.B., Dellai, J., 2007. Simulating the development of field grown potato (*Solanum tuberosum* L.). Agric. Meteorol. 142, 1–11. https://doi.org/10.1016/j.agrformet.2006.09.012.

Syrén, V., Wiik, L., 1993. Aktuellt om bladmögelbekämpning i potatis. Preparat, doser och intervall.

UN, 2015. Transforming our world: the 2030 Agenda for Sustainable Development.

Van der Plank, J.E., 1963. Plant diseases. Epidemics and Control. Academic Press, New York, USA.

Waggoner, P.E., Berger, R.D., 1987. Defoliation, disease, and growth. Phytopathology 77, 393–398.

Wallach, D., Makowski, D., Jones, J.W., Brun, F., 2019. Chapter 3 - Simulation with dynamic system models. In: Wallach, D., Makowski, D., Jones, J.W., Brun, F. (Eds.), Working with Dynamic Crop Models, Third edition.,. Academic Press, pp. 97–136. https://doi.org/10.1016/B978-0-12-811756-9.00003-4.

Wiik, L., 2014. Potato late blight and tuber yield: results from 30 years of field trials. Potato Res. 57, 77–98. https://doi.org/10.1007/s11540-014-9256-2.

Willocquet, L., Savary, S., Fernandez, L., Elazegui, F., Teng, P., 2000. Development and evaluation of a multiple-pest, production situation specific model to simulate yield losses of rice in tropical Asia. Ecol. Modell. 131, 133–159. https://doi.org/10.1016/S0304-3800(00)00271-4.

Willocquet, L., Savary, S., Fernandez, L., Elazegui, F.A., Castilla, N., Zhu, D., Tang, Q., Huang, S., Lin, X., Singh, H.M., Srivastava, R.K., 2002. Structure and validation of RICEPEST, a production situation-driven, crop growth model simulating rice yield response to multiple pest injuries for tropical Asia. Ecol. Modell. 153, 247–268. https://doi.org/10.1016/S0304-3800(02)00014-5.

Willocquet, L., Elazegui, F., Castilla, N., Fernandez, L., Fischer, K., Peng, S., Teng, P., Srivastava, R.K., Singh, H.M., Zhu, D., Savary, S., 2004. Research priorities for rice pest management in tropical Asia: a simulation analysis of yield losses and management efficiencies. Phytopathology 94 (7), 672–682.

Willocquet, L., Aubertot, J.N., Lebard, S., Robert, C., Lannou, C., Savary, S., 2008. Simulating multiple pest damage in varying winter wheat production situations. F. Crop. Res. 107, 12–28. https://doi.org/10.1016/j.fcr.2007.12.013.

Wolf, J., Van Oijen, M., 2003. Model simulation of effects of changes in climate and atmospheric CO_2 and O3 on tuber yield potential of potato (cv. Bintje) in the European Union. Agric. Ecosyst. Environ. 94, 141–157. https://doi.org/10.1016/S0167-8809(02)00029-4.

Wu, E.-J., Wang, Y.-P., Yahuza, L., He, M.-H., Sun, D.-L., Huang, Y.-M., Liu, Y.-C., Yang, L.-N., Zhu, W., Zhan, J., 2020. Rapid adaptation of the Irish potato famine pathogen *Phytophthora infestans* to changing temperature. Evol. Appl. 13, 768–780. https://doi.org/10.1111/eva.1289.

Yan, W., Hunt, L.A., 1999. An equation for modelling the temperature response of plants using only the cardinal temperatures. Ann. Bot. 84, 607–614. https://doi.org/10.1006/anbo.1999.0955.

Yang, L.-N., Zhu, W., Wu, E.-J., Yang, C., Thrall, P.H., Burdon, J.J., Jin, L.-P., Shang, L.-P., Zhan, J., 2016. Trade-offs and evolution of thermal adaptation in the Irish potato famine pathogen *Phytophthora infestans*. Mol. Ecol. 25, 4047–4058. https://doi.org/10.1111/mec.13727.

Yoshida, K., Schuenemann, V.J., Cano, L.M., Pais, M., Mishra, B., Sharma, R., Lanz, C., Martin, F.N., Kamoun, S., Krause, J., Thines, M., Weigel, D., Burbano, H.A., 2013. The rise and fall of the *Phytophthora infestans* lineage that triggered the Irish potato famine. Elife 2, e00731. https://doi.org/10.7554/eLife.00731.

Yuen, J.E., Andersson, B., 2013. What is the evidence for sexual reproduction of *Phytophthora infestans* in Europe? Plant Pathol. 62, 485–491. https://doi.org/10.1111/j.1365-3059.2012.02685.x.

Zadoks, J.C., Schein, R.D., 1979. Epidemiology and Plant Disease Management. Oxford University Press Inc., New York, USA.

Zhan, J., Thrall, P.H., Papaïx, J., Xie, L., Burdon, J.J., 2015. Playing on a pathogen's weakness: using evolution to guide sustainable plant disease control Strategies. Annu. Rev. Phytopathol. 53, 19–43. https://doi.org/10.1146/annurev-phyto-080614-120040.

Zhou, G., Wang, Q., 2018. A new nonlinear method for calculating growing degree days. Sci. Rep. 8, 10149. https://doi.org/10.1038/s41598-018-28392-z.

Zhou, Z., Plauborg, F., Kristensen, K., Andersen, M.N., 2017. Dry matter production, radiation interception and radiation use efficiency of potato in response to temperature and nitrogen application regimes. Agric. For. Meteorol. 232, 595–605. https://doi.org/10.1016/j.agrformet.2016.10.017.